

Final Report on Vacuum Drying of Grapes

Grapes, vacuum drying, moisture content, shrinkage, optimization

Digital Food Physics and Engineering BEE 4630/6630

Rachel Bocian, Isaiah Guenther, Wangqi Ma

May 11, 2023

Table of Contents

- [1. Executive Summary](#)
- [2. Introduction](#)
 - [2.1 Pretreatments](#)
 - [2.2 Vacuum Drying](#)
- [3. Results and Discussion](#)
- [4. Conclusions and Future Research](#)
- [5. Appendix A: Mathematical Statement of Problem](#)
- [6. Appendix B: Solution Strategy](#)
- [7. Appendix C: Additional Visuals](#)
- [8. References](#)

1. Executive Summary

The global market size for raisins was estimated to be \$2.6 billion in 2022 and is predicted to reach \$4 billion by 2030 (Wang et al., 2017). It is therefore critical to know and understand the process by which grapes are dried to raisins and what factors can be altered to optimize this process. The high water content of grapes leads to a low shelf life, making drying an ideal process for preservation. This drying process will be modeled using COMSOL to simulate the moisture loss and volume loss as a grape is dried to a raisin.

2. Introduction

2.1 Pretreatments

Grape skin presents a major obstacle to the drying process due to its low diffusivity which prevents moisture from leaving the pulp. The solution to this problem is to use a pretreatment on the grapes prior to drying in order to increase the drying rate. Two main categories of pretreatment exist: chemical and physical. Different pretreatments vary in the effect they have on skin diffusivity. Chemical pretreatments such as ethyl oleate and potassium carbonate create micro-fissures on the skin surface which leads to nonuniform skin removal, while physical pretreatment involves abrasion of the skin surface and results in uniform removal of the skin from the grape (Adiletta et al., 2016).

2.2 Vacuum Drying

Fruit has been commonly dried by convective drying with hot air, but vacuum drying has shown significant advantages since it presents a drying technique where moisture could be evaporated at low temperatures. By using a vacuum to dry the fruit, the initial shape is preserved and heat-sensitive compounds are not significantly damaged. Vacuum drying creates a low pressure and low moisture environment which speeds up the drying process by increasing the concentration gradient of water inside the grape and in the air.

3. Results and Discussion

Skin diffusivity of grapes is a parameter that can highly affect the drying process. In the modern food industry processes of grape drying, pretreatment of the grape skin is commonly and widely applied before drying the grapes. A good pretreatment process on the grape skin can successfully increase the skin diffusivity from approximately 10^{-20} m²/s to approximately 10^{-10} m²/s. Different affections of different skin diffusivities were studied during the research. As the model would be extremely complex, shrinkage was not considered in this case. By applying a parametric sweep with different skin diffusivities ranging from 10^{-10} m²/s to 10^{-22} m²/s, the moisture loss 1-D plot is shown in Appendix C (Fig 13). As it shows, without any pretreatments, it is nearly impossible to dry a grape in a reasonable time, while with proper pretreatments applied to the grapes, the moisture content can be dropped to a desired level in a much shorter time.

After proceeding through the drying process, the grapes will shrink because of moisture loss. This model simulated the shrinkage of the grape by assuming the volume of moisture loss equals the shrinkage of the grape. As a result, mesh velocity, which is the shrinking rate that is applied on the outer boundary of the grape skin, is the mass transfer flux divided by the density of water at the given condition. Under the condition of skin diffusivity = 10^{-10} m²/s and being dried for 4 hours, the model shows the final radius of the grape to be approximately 8.35 mm. The plot of radius change is shown in Appendix C (Fig 14), where the green line is a point at the full radius of the sphere, and the blue line marks the center, for reference.

Result validation was also applied to the shrinkage. Based on the literature, there is a linear mathematical model being retrieved to estimate the radius of a grape after being dried and shrinking (Simal et al., 1996). By plugging the data from the COMSOL model and the mathematical model from the literature into Excel, a graph containing the radius drop from both models was generated, and the root mean square error (RMSE) was calculated to indicate how those two datasets fitted with each other. The graph is shown in Appendix C (Fig 15), and the result RMSE value is 0.399 mm, which is considered to be an indication of high similarity between both models.

The validity of the entire model with shrinkage at a skin diffusivity of $10^{-10} \text{ m}^2/\text{s}$ was investigated by comparison to drying times from literature. Figure 1 below shows drying times for grapes in a vacuum dryer at different temperatures.

Drying Process	Temperature (°C)	Pressure	Drying Time (h)
Vacuum drying	35	100 mbar	12
Vacuum drying	50	100 mbar	5
Vacuum drying	70	100 mbar	3

Fig 1: grape drying times from Sokac et al., 2022

The grapes in Figure 1 were considered dry at 5-8% moisture content. Figure 2 shows the results when running the model at the drying time and associated temperature from literature.

Temperature (C)	Time Run (h)	Moisture Content (%)
35	6.45*	28.9
50	5	57.2
70	3	59.0

Fig 2: moisture content results of model grape after drying times from literature

**model was intended to run for 12 hours as reported, but crashed after 6.45 hours*

It can easily be seen that the model did not perfectly match real-world conditions. At a drying temperature of 35 °C, our model could not run to completion. At 50 °C and 70 °C, the model was able to finish running, but it did not reach the 5-8% moisture content level. There are a lot of possible explanations for this, but given the sake of time with the course, no investigation was done for improvement. However, the maximum run-times and resulting moisture content at each temperature was found and can be seen in the Figure 3 below. For 50 °C and 70 °C, 5-8% moisture content was reached, but this took longer than what is reported in literature. All time dependent studies were run with 0.1 hour intervals.

Temperature (C)	Max Time Ran (hr)	Moisture Content (%)
35	6.45	28.9
50	8.11	6.12
70	7.89	3.87

Fig 3: maximum run-times until crash and resulting moisture content

4. Conclusions and Future Research

After modeling the drying of a grape to a raisin using COMSOL software, results showed that an increase in temperature leads to an increase in the rate of drying. Additionally, an increase in skin diffusivity leads to an increase in the rate of drying which shows that pretreatment is necessary to dry grapes in a reasonable amount of time. This conclusion is valuable to the food industry as it allows for the optimization of time and resources. Cost analysis may be performed to analyze whether the increased cost of performing a pretreatment is worth the time saved during drying. It was also concluded that the rate of shrinkage is a linear function, and that the rate of drying is nearly linear when shrinkage is included in the model. Because the model was unable to run for diffusivities below $10^{-12} \text{ m}^2/\text{s}$, in the future the model should be used to analyze all diffusivities in order to encompass the entire pre-treated and untreated range of diffusivities. Input values may also be adjusted to represent different grape varieties in order to create models specific to the grape of interest.

5. Appendix A: Mathematical Statement of Problem

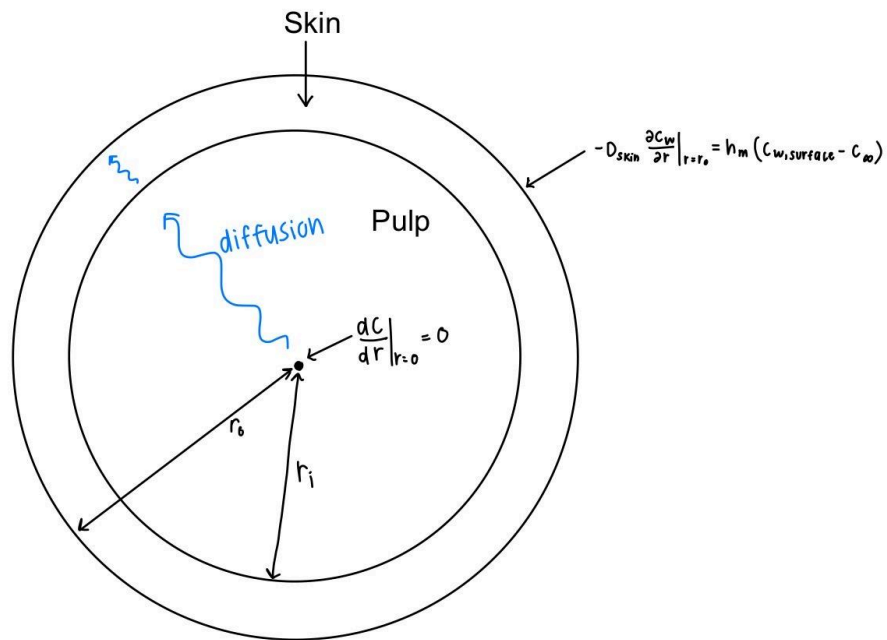


Fig 4: schematic of grape drying problem

$$\frac{\partial c_A}{\partial t} = D_{AB} \frac{1}{r^2} \frac{\partial}{\partial r} \left(r^2 \frac{\partial c_A}{\partial r} \right)$$

Eqn 1: governing equation for mass transfer of water through grape

$$\left. \frac{dC}{dr} \right|_{r=0} = 0$$

Eqn 2: zero flux boundary condition at center of grape

$$-D_{skin} \left. \frac{\partial c_A}{\partial r} \right|_{r=r_o} = h_m (c_{A, surface} - c_{\infty}) = h_m \left(\frac{P_v a_w}{RT} - c_{\infty} \right)$$

Eqn 3: convective boundary condition at surface of grape

$$c_A = 53913.737 \frac{\text{mol}}{\text{m}^3}$$

Eqn 4: initial water concentration of grape

A	1e-3[m^2]
c_inf	.036 [mol/m^3]
d	1000[kg/m^3]
D_skin	10^-16[m^2/s]
D0	0 [m^2/s]
Di	5.35*10^-9[m^2/s]
E0	10400[J/mol]
Ei	34000[J/mol]
h_m	10^-3 [m/s]
M	.018[kg/mol]
mass_dry	9.35*10^-4 [kg]
P_vw	19937[J/m^3]
R.	8.314[m^3*Pa/K/mol]
T.	333[K]
Tr	333[K]
V	3.351*10^-5[m^3]

Table 1: all input parameters

$$D = \frac{1}{1+X} D_o \exp \left[-\frac{E_o}{R} \left(\frac{1}{T} - \frac{1}{T_r} \right) \right] + \frac{X}{1+X} D_i \exp \left[-\frac{E_i}{R} \left(\frac{1}{T} - \frac{1}{T_r} \right) \right]$$

Eqn 5: pulp diffusivity

X	a_w
0.05	0.05
0.14	0.3
0.175	0.41
0.18	0.5
0.19	0.56
0.275	0.7
0.3	0.75
0.41	0.88

Table 2: water activity

6. Appendix B: Solution Strategy

The solution was implemented using COMSOL's Transport of Diluted Species (tds) physics in the 2D-Axisymmetric model wizard as a time-dependent study. The geometry was built using COMSOL's difference feature between two half circles. A 10mm half circle was cut by an overlaid 9.998mm half circle to create one half circle with two different regions. The inner region represented the pulp of the grape, from 0.0mm to 9.998mm, while the outer 2.0µm represented the grape skin:

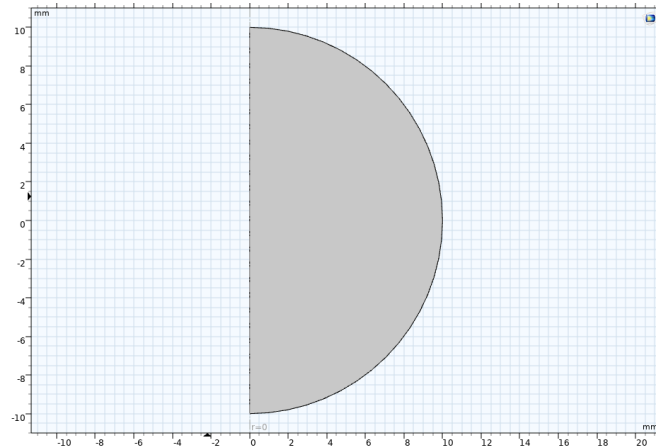


Fig 5: complete view of grape pulp and skin

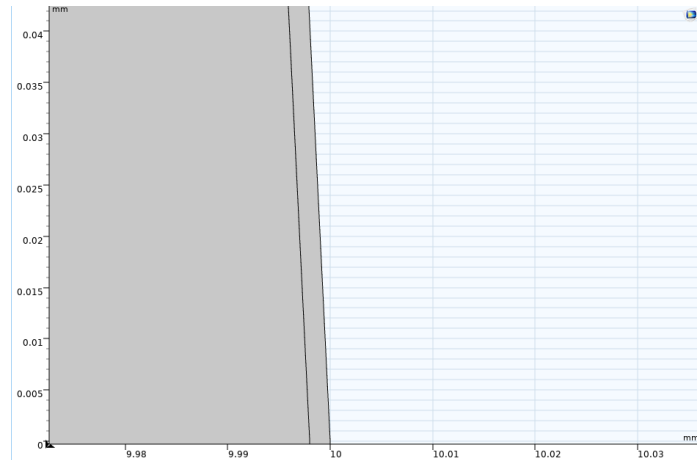


Fig 6: zoomed-in view of grape skin

The convective flux boundary condition was applied on the outermost layer of the skin:

$$J_{0,c} = -h_m \cdot ((P_{vw} \cdot a_w(c \cdot V \cdot M / \text{mass_dry})) / (R \cdot T)) - c_{\text{inf}} \quad \text{mol}/(\text{m}^2 \cdot \text{s})$$

By default, the 2D-Axisymmetric model wizard applies a no-flux boundary condition on the axis of symmetry, satisfying our second boundary condition.

The diffusivity equation above was applied to the pulp region, while different constant values were applied to the skin. Isothermal water activity as a function of moisture content was implemented through piecewise cubic interpolation and constant extrapolation using data from literature:

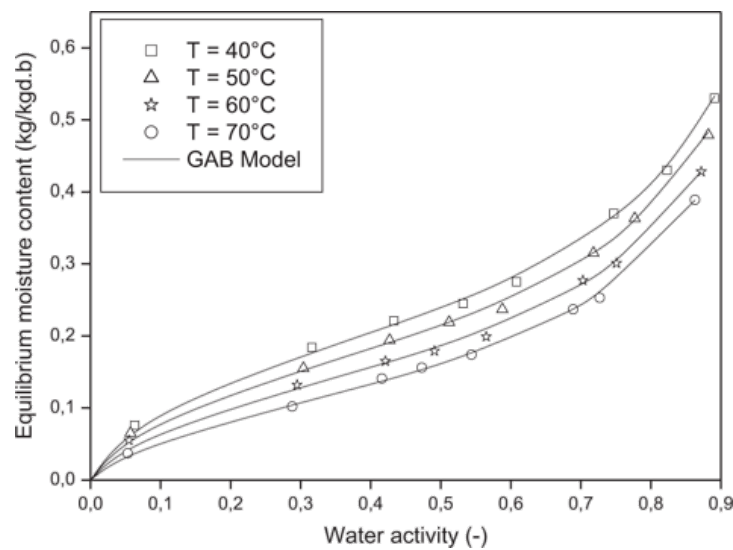


Fig 7: water activity data from Hermassi et. al

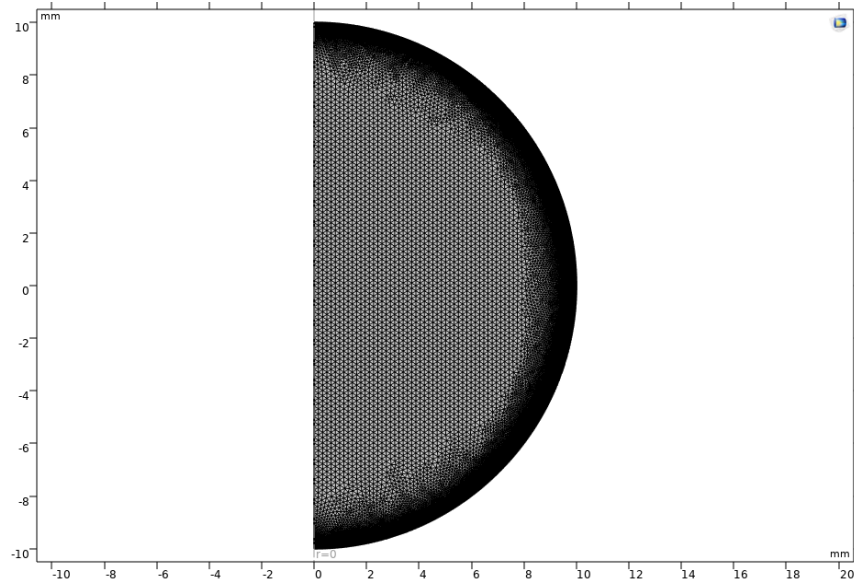


Fig 8: extremely fine mesh at $t = 0$ s

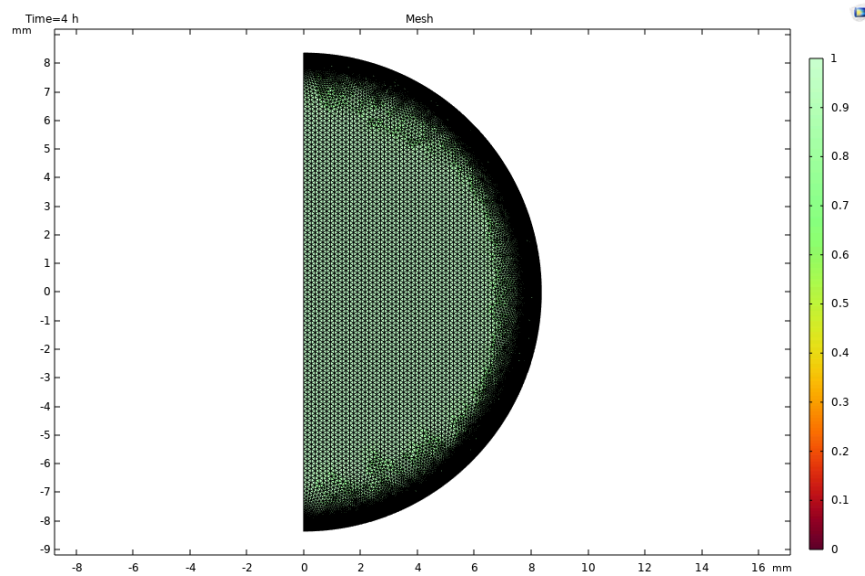


Fig 9: extremely fine mesh at $t = 4$ hours

Figure 8 above is the mesh that was used for the grape. In the beginning, the Extremely Fine mesh was constructed in order to make it as precise as possible to simulate the mass transfer of moisture. Figure 9 is the mesh after a time-dependent study of 4 hours. As it shows, the mesh became compressed, but can still form a reasonable structure. In order to save time in modeling, a mesh convergence step was applied to the model. Several other meshes at different fineness were tried. After several trials and comparisons between the results of the new-mesh model and the original one, an extremely coarse mesh was chosen to do the mesh convergence. Below are the figures of the extremely coarse mesh when $t = 0$ s and $t = 4$ hours. Also, the plots of moisture

change in respect of time for both the extremely fine mesh and the extremely coarse mesh are listed. As they show, compared to the extremely fine mesh model, the extremely coarse mesh model has a result of high similarity and a much lower computing time.

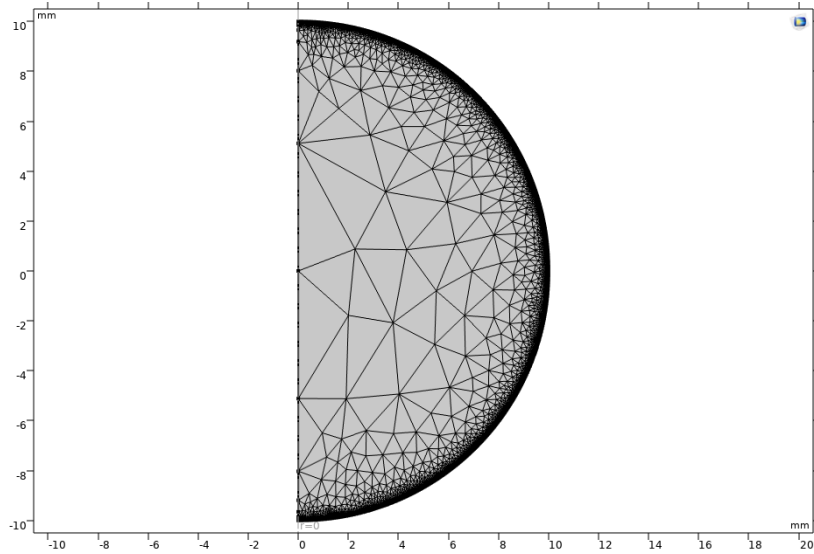


Fig 10: extremely coarse mesh at $t = 0$ s

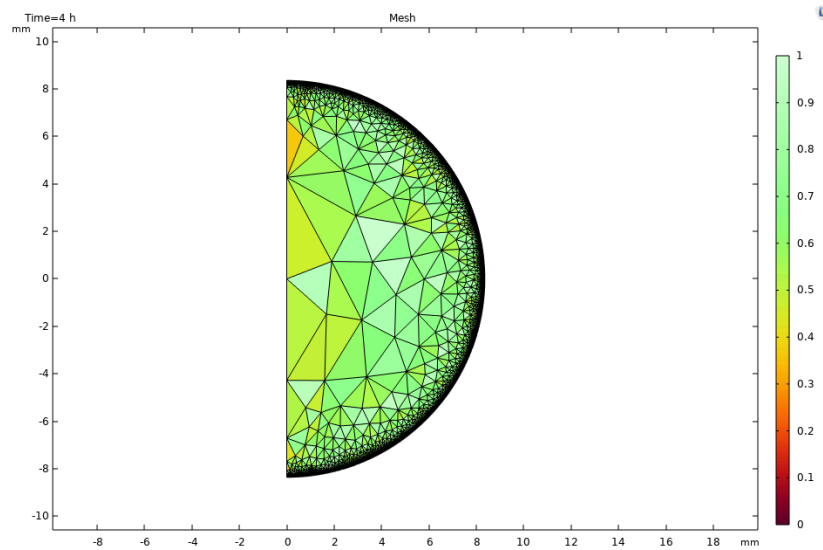


Fig 11: extremely coarse mesh at $t = 4$ hours

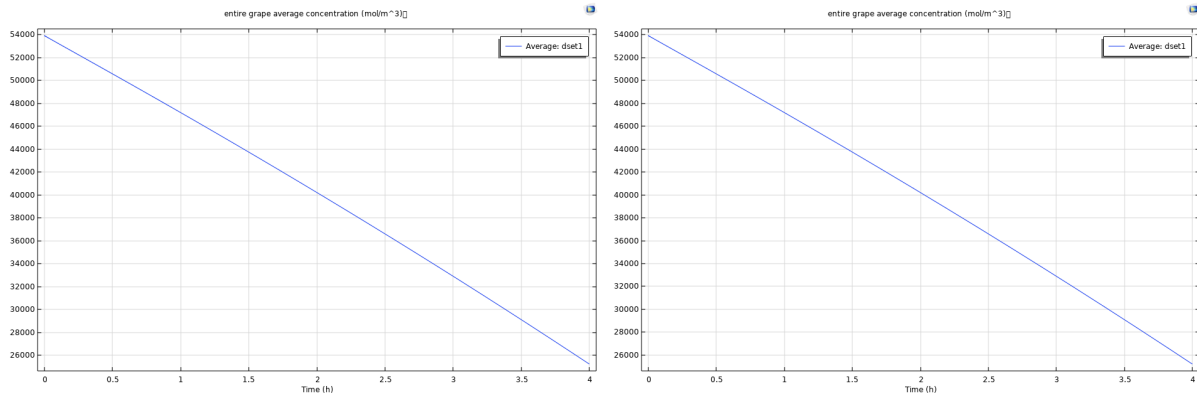


Fig 12: moisture vs time plots for extremely fine (left) and extremely coarse (right)

7. Appendix C: Additional Visuals

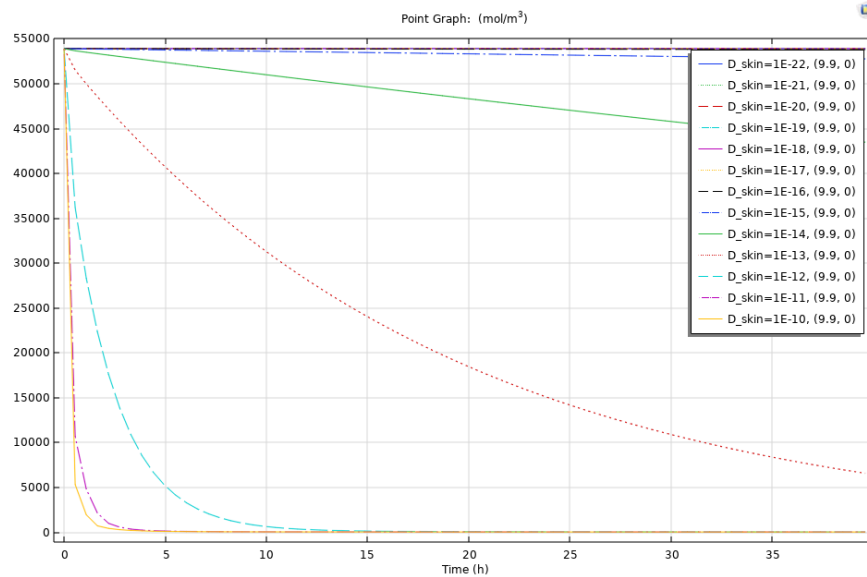


Fig 13: moisture loss vs time with different skin diffusivities

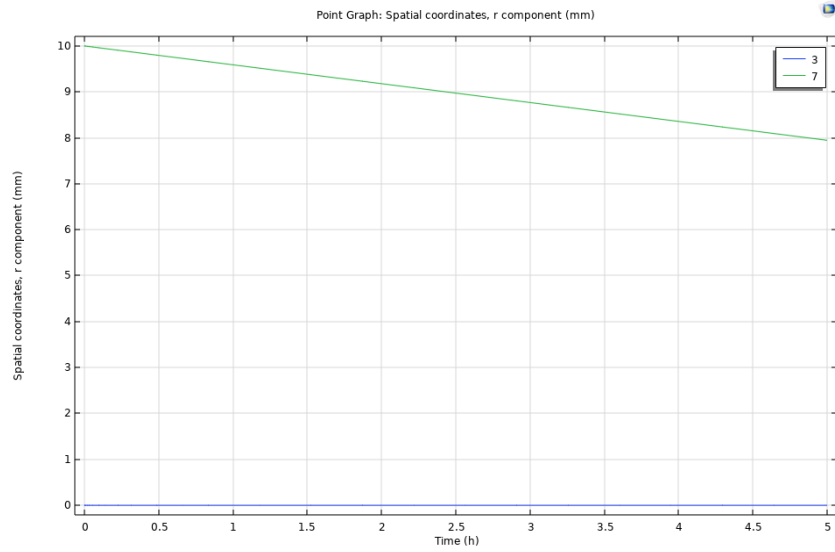


Fig 14: plots of radius change caused by shrinkage

Radius vs. Concentration for Shrinking

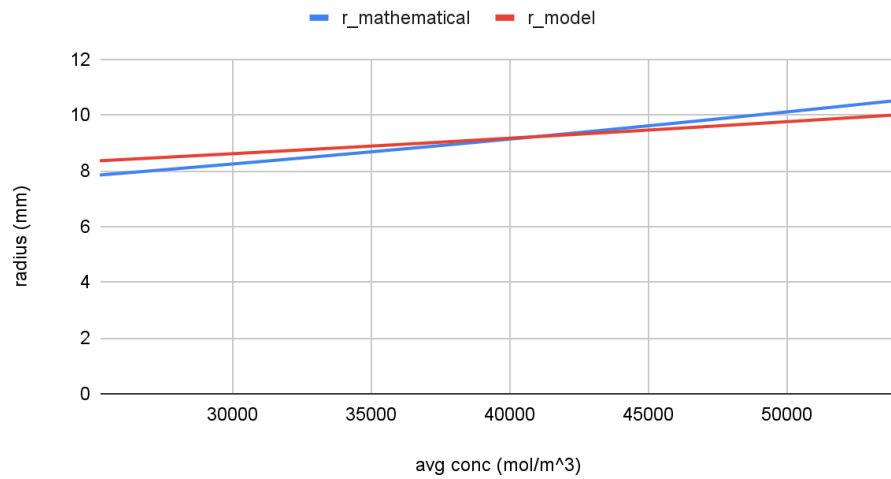


Fig 15: graph for shrinkage from two models

8. References

- Adiletta, G., Russo, P., Senadeera, W., & Di Matteo, M. (2016). Drying characteristics and quality of grape under physical pretreatment. *Journal of Food Engineering*, 172, 9–18.
<https://doi.org/10.1016/j.jfoodeng.2015.06.031><https://doi.org/10.1016/j.fbp.2017.09.003>
- Simal, S., Mulet, A., Catalá, P. j., Cañellas, J., & Rosselló, C. (1996). Moving Boundary Model For Simulating Moisture Movement In Grapes. *Journal of Food Science*, 61(1), 157–160.
<https://doi.org/10.1111/j.1365-2621.1996.tb14748.x>
- Wang, J., Mu, W.-S., Fang, X.-M., Mujumdar, A. S., Yang, X.-H., Xue, L.-Y., Xie, L., Xiao, H.-W., Gao, Z.-J., & Zhang, Q. (2017). Pulsed vacuum drying of Thompson seedless grape: Effects of berry ripeness on physicochemical properties and drying characteristic. *Food and Bioprocess Processing*, 106, 117–126.
<https://doi.org/10.1016/j.fbp.2017.09.003>
- Deer, T. W. W., and J. R. Whiting. “Evaluation of Sultana Grapevine Selections for Table Grape Production.” *Australian Journal of Experimental Agriculture* 29, no. 6 (1989): 901–4. <https://doi.org/10.1071/ea9890901>.
- Esmaili, Mohsen, Rahmat Sotudeh-Gharebagh, Kevin Cronin, Mohammad Ali E. Mousavi, and Ghader Rezazadeh. “Grape Drying: A Review.” *Food Reviews International* 23, no. 3 (June 22, 2007): 257–80. <https://doi.org/10.1080/87559120701418335>.
- Hermassi, Imène, Sofien Azzouz, Lamine Hassini, and Ali Belghith. “Moisture Diffusivity of Seedless Grape Undergoing Convective Drying.” *Chemical Product and Process Modeling* 12, no. 1 (March 1, 2017). <https://doi.org/10.1515/cppm-2016-0074>.
- ReportLinker. “Global Raisins Market to Reach \$4 Billion by 2030.” GlobeNewswire News Room, May 8, 2023.
<https://www.globenewswire.com/news-release/2023/05/08/2663755/0/en/Global-Raisins->

[Market-to-Reach-4-Billion-by-2030.html](#).

Saravacos, George D., and Zacharias B. Maroulis. *Transport Properties of Foods*. 0 ed. CRC Press, 2001. <https://doi.org/10.1201/9781482271010>.

Sokač, Tea, Veronika Gunjević, Anita Pušek, Ana Jurinjak Tušek, Filip Dujmić, Mladen Brnčić, Karin Kovačević Ganić, et al. “Comparison of Drying Methods and Their Effect on the Stability of Graševina Grape Pomace Biologically Active Compounds.” *Foods* 11, no. 1 (January 2022): 112. <https://doi.org/10.3390/foods11010112>.

Šuklje, Katja, Klemen Lisjak, Helena Baša Česnik, Lucija Janeš, Wessel Du Toit, Zelmari Coetzee, Andreja Vanzo, and Alain Deloire. “Classification of Grape Berries According to Diameter and Total Soluble Solids To Study the Effect of Light and Temperature on Methoxypyrazine, Glutathione, and Hydroxycinnamate Evolution during Ripening of Sauvignon Blanc (*Vitis Vinifera* L.).” *Journal of Agricultural and Food Chemistry* 60, no. 37 (September 19, 2012): 9454–61. <https://doi.org/10.1021/jf3020766>.